

# Thermal decomposition of hydrotalcite-like compounds studied by a novel tapered element oscillating microbalance (TEOM) Comparison with TGA and DTA

Javier Pérez-Ramírez<sup>a,b,\*</sup>, Sònia Abelló<sup>a</sup>

<sup>a</sup> Institute of Chemical Research of Catalonia (ICIQ), Av. Països Catalans 16, E-43007 Tarragona, Spain

<sup>b</sup> Catalan Institution for Research and Advanced Studies (ICREA), Pg. Lluís Companys 23, E-08010 Barcelona, Spain

Received 2 February 2006; received in revised form 14 February 2006; accepted 23 February 2006

## Abstract

For the first time, we report on the application of a tapered element oscillating microbalance (TEOM) as a novel technique to investigate the thermal decomposition of hydrotalcite-like compounds (HTLcs) in air. Experiments were performed in the temperature range of 323–973 K with Mg–Al, Ni–Al, and Co–Al-HTLcs. The TEOM technique measures mass changes based on inertial forces, presenting important advantages over conventional thermogravimetric analyzers, such as the very rapid time response and the well-defined flow pattern. In general terms, excellent agreement between TEOM, TGA, and DTA techniques during HTLc decomposition was obtained. Interestingly, transition temperatures in the TEOM were lower than in TGA and DTA, particularly for removal of interlayer water but also for dehydroxylation of the brucite-like layers and decarbonation. This was attributed to the flow-through operation in the tapered element of the TEOM as compared to the recognized gas stagnancy and bypass in sample crucibles of conventional thermogravimetric analyzers. Our results conclude that the TEOM technique is suitable for temperature-programmed studies. However, due to its operation principle, blank runs are required in contrast to the more automatic operation in commercial thermogravimetric units. Besides, a careful sample loading and packing in the micro-reactor is essential for reproducible results. © 2006 Elsevier B.V. All rights reserved.

**Keywords:** Tapered element oscillating microbalance; TEOM technique; TGA; DTA; Clays; Hydrotalcites; Thermal decomposition

## 1. Introduction

Synthetic hydrotalcite-like compounds (HTLcs), also referred to as anionic clays or Feitknecht's compounds, are mixed hydroxides of lamellar structure with a general formula  $[M_{1-x}^{2+}M_x^{3+}(\text{OH})_2][X^{n-}]_{x/n}\cdot m\text{H}_2\text{O}$ . As outlined by Allman [1] and Taylor [2], these materials can be visualized as brucite-type octahedral layers, in which  $M^{3+}$  cations partially substitute for  $M^{2+}$  cations. The positive charge resulting from this substitution is balanced by anions (often carbonate) and water molecules arranged in interlayers in alternation with the octahedral layers (Fig. 1).

HTLcs have attracted much attention in recent years as catalyst precursors due to the ability of these materials to accommodate a large variety of divalent and trivalent cations, and the formation

of high-surface area and well-dispersed mixed oxides [3]. The catalytic properties of the HTLc-derived mixed oxides largely depend on the activation procedure [4] and thus monitoring structural changes during thermal decomposition of hydrotalcites has been the aim of numerous studies. Thermal analysis using conventional thermogravimetric techniques coupled with DTA or DSC has been the most widely used method to investigate the transitions involved during hydrotalcite decomposition. Patterns are characterized by a two-step mass loss behaviour with two endothermic transitions associated with the sequential loss of interlayer water in the first step (<473 K) followed by the combined dehydroxylation of the brucite-like layers and decarbonation in the second step. The transition temperature for the latter step, which leads to the collapse of the layered structure, depends on the composition of the hydrotalcite (e.g. ca. 523, 623, and 683 K for Co–Al, Ni–Al, and Mg–Al-HTLcs, respectively [5]). To accurately describe the decomposition mechanism of HTLcs, multi-technique in situ approaches have been applied, including TGA–DTA–DSC coupled to MS analysis of

\* Corresponding author. Tel.: +34 977 920 236; fax: +34 977 920 224.  
E-mail address: [jperez@iciq.es](mailto:jperez@iciq.es) (J. Pérez-Ramírez).

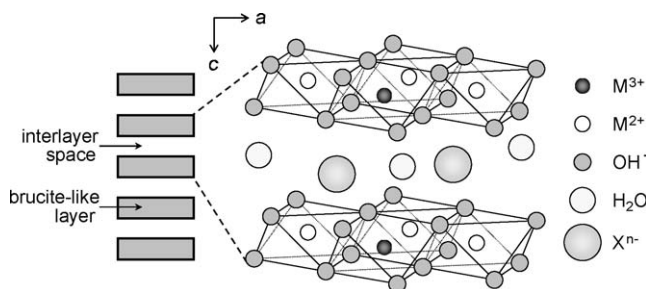


Fig. 1. Representation of the hydrotalcite structure.

the decomposition products, HT-XRD, and FT-IR and Raman spectroscopies [6–9].

A novel tapered element oscillating microbalance (TEOM) can be proposed as a suitable complementary technique to the above-mentioned approaches, particularly as an alternative to TGA–DTA–DSC, to assess HTlc decomposition. The TEOM microbalance presents improvements with respect to thermogravimetric analyzers (Fig. 2): a well-defined flow-through profile, eliminating bypass problems and possible (heat and mass) diffusion and buoyancy phenomena in contrast to flow around and over the sample crucible in conventional microbalances, and a very fast response time resolution (0.1 s) allowing the study of processes with fast kinetics. These are key features for the successful application of the TEOM technique in adsorption, absorption, diffusion, desorption, release, reaction, and coking studies [10–16]. However, to the best of our knowledge, published works with this microbalance are mainly confined to isothermal operation, i.e. temperature-programmed investigations are scarce. Exceptionally, some of us reported temperature-programmed oxidation (TPO) in order to determine coke burn-off in iron-zeolites after  $N_2O$ -mediated propane oxidative dehydrogenation [17].

In this work, we have applied the tapered element oscillating microbalance (TEOM) as a novel technique to investigate the thermal decomposition of Mg–Al, Ni–Al, and Co–Al hydro-

talcsites in air. TEOM results have been compared with those obtained by well-established TGA and DTA techniques.

## 2. Experimental

### 2.1. Materials

The  $M^{2+}$ –Al hydrotalcites with a molar  $M^{2+}/Al$  ratio of 3 ( $M^{2+} = Mg, Ni, Co$ ) were prepared by coprecipitation, starting from an aqueous solution of the respective metal nitrates  $Mg(NO_3)_2 \cdot 6H_2O$  (0.75 M),  $Ni(NO_3)_2 \cdot 6H_2O$  (0.75 M),  $Co(NO_3)_2 \cdot 6H_2O$  (0.75 M) and  $Al(NO_3)_3 \cdot 9H_2O$  (0.25 M) and an aqueous solution of  $NaOH/Na_2CO_3$  (2 M). Ni–Al-HTlc-1, Ni–Al-HTlc-2, Mg–Al-HTlc-1, and Co–Al-HTlc-1 were coprecipitated at constant pH ( $10 \pm 0.2$ ) by adding dropwise the solutions of cations and anions to the precipitation vessel under stirring at 298 K. The resulting slurries were aged under vigorous stirring at 298 K (333 K for Ni–Al-HTlc-2) during 15 h. Finally, the materials were filtered, washed with a large amount of deionized water, and dried at 363 K for 12 h. Ni–Al-HTlc-3 was coprecipitated at decreasing pH, i.e. adding the solution of cations to the solution of anions until pH 10. Mg–Al-HTlc-2 was obtained by thermal decomposition of Mg–Al-HTlc-1 at 798 K for 15 h, followed by reconstruction in decarbonated water at 298 K for 1 h, filtration, washing with ethanol, and finally drying in flow argon at room temperature.

The chemical composition of the as-synthesized materials was determined by inductive coupled plasma-optical emission spectroscopy (ICP-OES) (Perkin-Elmer 40 (Si) and Optima 300DC (axial)). Powder X-ray diffraction was measured in a Siemens D5000 diffractometer with Bragg–Brentano geometry and  $Cu K\alpha$  radiation ( $\lambda = 0.1541$  nm). Data were collected in the  $2\theta$  range of  $5\text{--}65^\circ$  using a step size of  $0.05^\circ$  and a counting time of 8 s. Scanning Electron Microscopy was recorded at 5 kV in a JEOL JSM-6700F field-emission microscope. Samples were coated with palladium to create contrast.

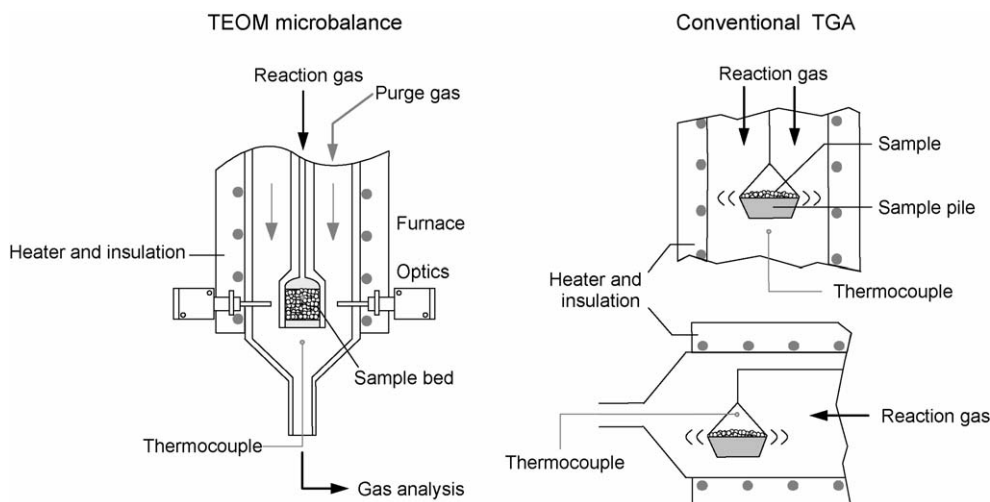


Fig. 2. Drawing of the TEOM microbalance and comparison with conventional thermogravimetric analyzers.

## 2.2. TGA–DTA experiments

Thermal analysis was carried out in a Mettler Toledo TGA/SDTA851e microbalance equipped with a 34-positions sample robot. The solid (20 mg, sieve fraction 125–200  $\mu\text{m}$ ) was diluted with silicon carbide (100 mg, sieve fraction 125–200  $\mu\text{m}$ ) and placed in alumina sample crucibles (70  $\mu\text{l}$ ). Analyses were performed in dry air flow of 100  $\text{cm}^3$  (STP)  $\text{min}^{-1}$ . The temperature was increased from 323 to 973 K applying heating rates of 2, 5, 10, and 15  $\text{K min}^{-1}$ .

## 2.3. TEOM experiments

### 2.3.1. Apparatus and principle of the technique

A Rupprecht and Patashnick TEOM 1500 mass analyzer was used for investigating the thermal decomposition of hydrotalcites. The TEOM consists of a micro-reactor (4 mm i.d.) with a high resolution microbalance that generates real-time measurements of mass changes during gas–solid interactions (Fig. 2). Its operation principle is based on inertial forces and has been described in detail elsewhere [10–12]. Briefly, the active element of the TEOM consists of a tapered tube of proprietary glass material that can be set to vibrate at its harmonic frequency of oscillation (ca. 70 Hz). When the mass of the material test bed increases, the natural oscillating frequency of the tapered element decreases, and vice versa. By comparing the measured frequency to the one stored at the beginning of the experiment, the system acquires an accurate and time-resolved record of mass changes, since the frequency of a harmonic oscillator is directly proportional to its mass. If the TEOM is oscillating to start at the frequency of  $f_0$  and exhibits a frequency  $f_1$  after a mass uptake, the total mass change ( $\Delta m$ ) can be obtained as a function of  $f_0$ ,  $f_1$ , and the spring constant  $K_0$ :

$$\Delta m_t = \Delta m_s + \Delta m_g = K_0 \left( \frac{1}{f_1^2} - \frac{1}{f_0^2} \right) \quad (1)$$

The principle for detecting frequencies is by a light emitting diode–phototransistor combination, and the light blocking effect of the vibrating element. Based on the operation principle of the TEOM, the total mass uptake is the sum of the mass change of the sample ( $\Delta m_s$ ) and the change in the gas density ( $\Delta m_g$ ). The change in the gas density depends on the type of gas and the operating conditions. In order to correct for this, blank experiments have to be performed, as described below.

### 2.3.2. Operating procedures

The TEOM micro-reactor was carefully loaded with 20 mg of sample and 100 mg of silicon carbide. As explained in Section 3.3, sample dilution by inert particles was required in order to obtain reproducible results. The sample and diluent particles (sieve fraction 125–200  $\mu\text{m}$ ) were well mixed before introducing them in the reactor tube. Quartz wool was used at the top and the bottom of the sample bed to keep the adsorbent particles firmly packed, which is also essential for a stable measurement. The material was pre-treated in flowing dry air according to the following temperature program (Fig. 3a): heating from room

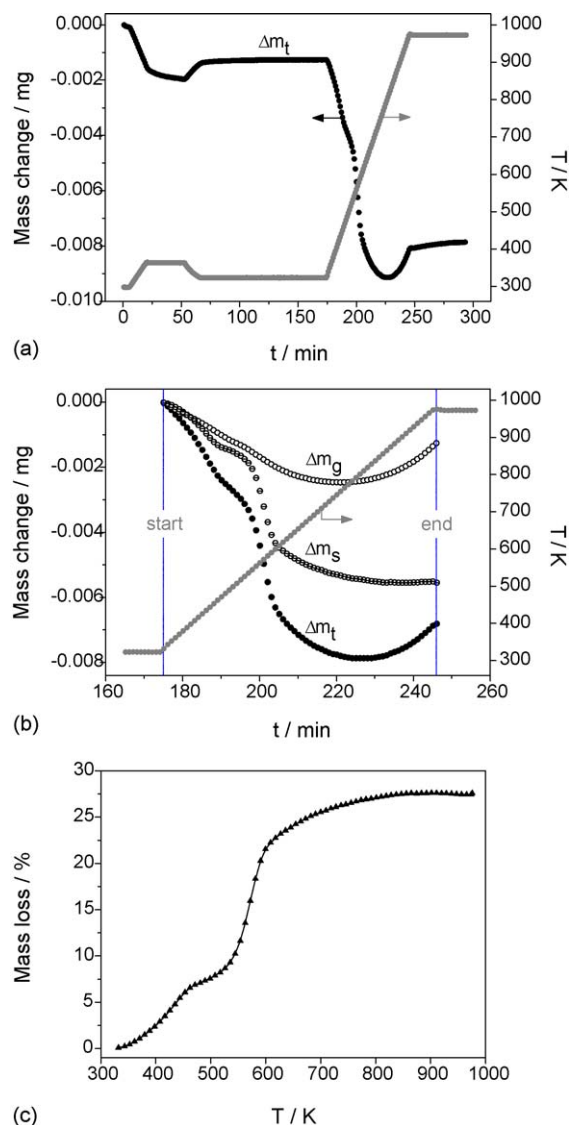


Fig. 3. Procedure to determine mass loss (c) during HTlc decomposition from the measurement of the total mass change (a),  $\Delta m_t$ ,  $\Delta m_s$  and  $\Delta m_g$  in (b) refer to mass changes due to the sample and the changes in gas density during the temperature ramp, respectively.

temperature to 363 K and hold for 30 min to remove physically adsorbed water from the sample, followed by a decrease to 323 K. When a stable baseline was attained, the temperature was ramped from 323 to 973 K at different heating rates (2, 5, 10, and 15  $\text{K min}^{-1}$ ) and total mass changes ( $\Delta m_t$ ) were continuously monitored. Equal flows of purge gas (He) and reaction gas (air) of 100  $\text{cm}^3$  (STP)  $\text{min}^{-1}$  were used and the temperature of the feed gases were set to 323 K. All experiments were performed without thermocouple in the catalyst bed, since it led to unsatisfactory mass data.

In order to determine mass changes due to the sample ( $\Delta m_s$ ), the total mass change has to be corrected for the contribution of changes in density due to the temperature ramp. To this end, the response of the TEOM was measured without sample at the same conditions of gas composition, flow in the carrier and purge lines, and temperature program, leading to the signal  $\Delta m_g$

in Fig. 3b. Three different blank runs were performed: with the empty reactor, with the reactor filled with quartz wool, and with the reactor filled with SiC particles (sieve fraction 125–200  $\mu\text{m}$ ) sandwiched between two plugs of quartz wool. No appreciable differences were observed in the mass changes among them. The mass change due to the sample ( $\Delta m_s$ ) can be determined by subtracting the profiles of  $\Delta m_t$  and  $\Delta m_g$ , and this magnitude can be expressed as the percentage of mass loss using Eq. (2), where  $m_o$  is the sample mass loaded in the TEOM micro-reactor. The final outcome of the TEOM data processing is shown in Fig. 3c.

$$\text{mass loss} = \frac{\Delta m_s}{m_o} \times 100. \quad (2)$$

### 3. Results and discussion

#### 3.1. Materials characterization

Elemental chemical analysis data of all samples indicated that the molar metal ratio in the solids was very close to the value in the parent solutions, i.e.  $M^{2+}/\text{Al} = 3/1$  with  $M^{2+} = \text{Mg}$ , Co, Ni. This means that the precipitation step was carried out effectively. Fig. 4 shows the XRD patterns of the as-synthesized HTlcs. All samples show the hydroxalcalite structure as the only crystalline component (JCPDS 22-700) exhibiting sharp and symmetric reflections for the basal (003), (006), and (009) planes, and broad and asymmetric reflections for the non-basal (012), (015), and (018) planes. The overlap of the (009) and (012) reflections results in a broad signal between  $32^\circ$  and  $38^\circ$   $2\theta$ . The typical (110) and (113) reflections can also be clearly distinguished.

As exemplified by the SEM micrograph of Ni–Al-HTlc-1 in Fig. 5, all the as-synthesized samples exhibited the characteristic morphology of well-developed and disordered platelets. The lateral size of these platelets is in the range of 8–20 nm, basically depending on the nature of the divalent cations and preparation procedure.

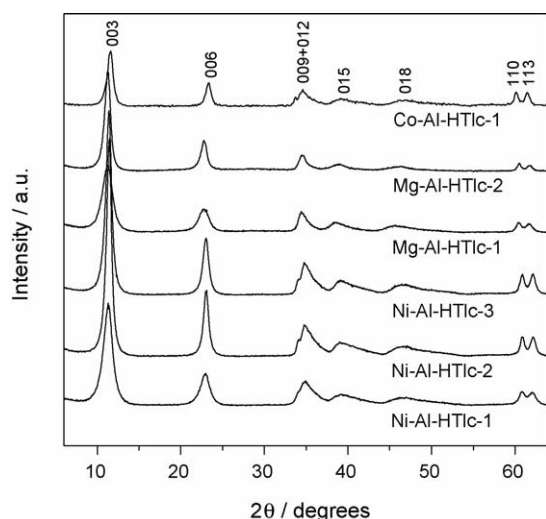


Fig. 4. XRD patterns of the as-synthesized hydroxalcalcites.

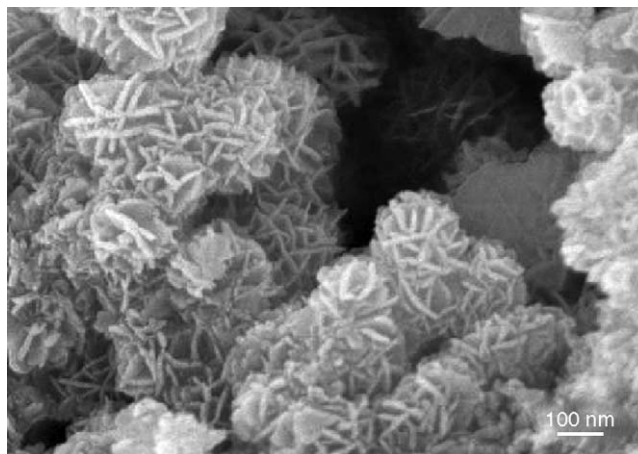


Fig. 5. SEM micrograph of Ni–Al-HTlc-1.

#### 3.2. Mass loss profiles

The profiles of mass loss versus temperature during air-decomposition of the hydroxalcalite-like compounds as determined by TEOM and TGA microbalances are shown in Fig. 6. All the samples display the two-step decomposition behaviour reported for HTlcs [18]. The first step of mass loss (<500 K) amounts ca. 10–15% and corresponds to the removal of interlayer water molecules (dehydration). In the applied program, samples were intentionally pre-treated in air flow at 363 K for 30 min in order to minimize losses by physically adsorbed water during the temperature ramp. The second mass loss (500–773 K) is associated with the removal of water by dehydroxylation of the brucite-like sheets and decomposition of compensating carbonate anions in the interlayer space. Above 773 K, a gradual mass loss is still observed as a consequence of the slow removal of residual carbonates in the samples. As shown in Table 1, the transition temperature for interlayer water removal (denoted as  $T_1$ ) is within a narrow range independently of divalent cation in the structure and preparation method (426–458 K according to the derivative of TEOM mass loss data). However, the transition temperature for dehydroxylation and decarbonation strongly depends on the composition of the brucite-like sheets. Based on

Table 1  
Transition temperatures for the decomposition of the hydroxalcalite samples in air as determined by TEOM, TGA, and DTA techniques

Sample	$T_1^a$ (K)			$T_2^b$ (K)		
	TEOM	TGA	DTA	TEOM	TGA	DTA
Co–Al-HTlc-1	445	471	472	509	512	518
Ni–Al-HTlc-1	444	473	479	581	582	582
Ni–Al-HTlc-2	450	479	485	606	615	621
Ni–Al-HTlc-3	458	479	485	595	615	621
Mg–Al-HTlc-1	426	455	460	664	668	668
Mg–Al-HTlc-2	452	478	485	635	650	654

Heating rate = 10 K  $\text{min}^{-1}$

<sup>a</sup>  $T_1$ : dehydration.

<sup>b</sup>  $T_2$ : dehydroxylation and decarbonation.



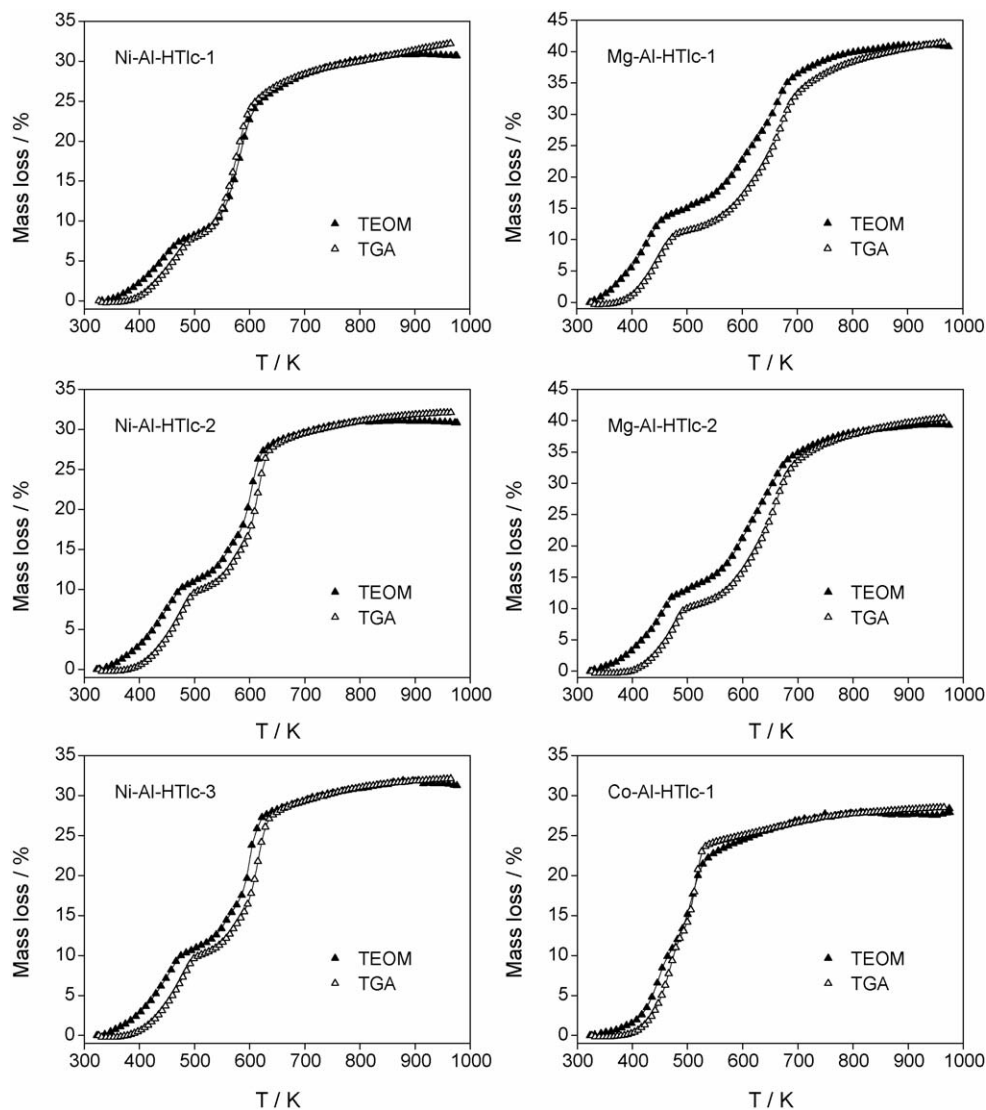


Fig. 6. Comparison between TEOM and TGA profiles during thermal decomposition of HTlcs with different metals and preparation methods. Heating rate =  $10 \text{ K min}^{-1}$ .

TEOM data, the thermal stability of Mg–Al-HTlc-1 ( $T_2 = 664 \text{ K}$ ) is higher than that of Ni–Al-HTlc-1 ( $T_2 = 581 \text{ K}$ ) and Co–Al-HTlc-1 ( $T_2 = 509 \text{ K}$ ). The stability order agrees well with that determined in the literature using various techniques [5,7]. The total mass loss of the samples as derived from Fig. 6 (ca. 28% in Co–Al, ca. 30% in Ni–Al, and ca. 40% in Mg–Al hydrotalcites) is also in line with reported values on these materials [7,9]. As displayed in Table 1, the  $T_1$  values in the Ni–Al hydrotalcites are very similar, while  $T_2$  values are somewhat different (lower in Ni–Al-HTlc-1) due to the preparation method. It is interesting to observe that interlayer water is more stable in reconstructed Mg–Al-HTlc-2 (with hydroxyl groups as compensating anions) as compared to the as-synthesized Mg–Al-HTlc-1 (with carbonate groups as compensating anions), while the opposite occurs for the dehydroxylation process leading to the collapse of the layered structure. It is out of the scope of this paper to discuss in detail transition temperature variations in the differently prepared samples. Rather, it should be stressed that the three

techniques provide the same trends over samples with different genesis and composition. Fig. 6 enables us to generally conclude that there is excellent correspondence between TEOM and TGA with respect to the mass losses, and the shift of the mass loss profiles in the TEOM microbalance, leading to lower transition temperatures (see also Table 1). The latter result is not a consequence of a temperature effect in the TEOM and TGA microbalances, as the T-controllers in both instruments were properly calibrated so as to achieve identical profiles during the temperature program. This aspect will be further discussed in Section 3.4.

### 3.3. Technique reproducibility

The experiments in Fig. 6 were repeated several times in both TEOM and TGA–DTA systems in order to assess the reproducibility of the methods. TGA–DTA yielded excellent repeatability. The TEOM technique was reproducible too, but

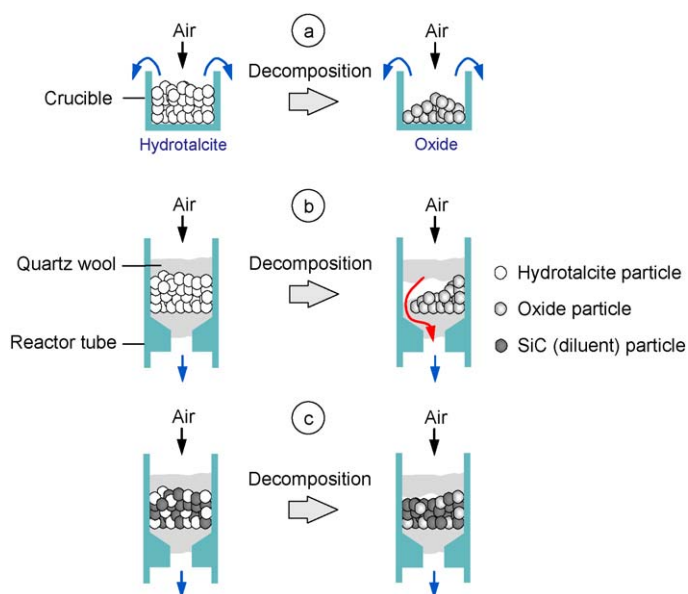


Fig. 7. Sample dilution with inert particles is essential to obtain stable and reproducible mass data during thermal decomposition studies with the TEOM.

developing proper procedures for reactor loading and packing was necessary. In conventional thermal analyzers (Fig. 7a), the initial sample mass can be easily determined by weighing the crucible before and after loading the sample. Some of the commercial models, like the one used in this study, have automatic weighing built in. Besides, the mass measurement was found to be unaffected by possible uneven distribution of particles in the crucible as a consequence of the change in sample volume (decreasing, due to decomposition).

In the TEOM, extreme care has to be taken for loading the solid sample in the micro-reactor, as a minor sample loss (e.g. powder sticking to the wall of the capsule used for sample weighing) can lead to significant errors in mass loss determination by overestimating the initial sample amount. For example, not transferring just 2 mg to the TEOM micro-reactor out of the 20 mg originally weighed represents an error in the initial mass of 10%. Accordingly, accurate operation for sample weighing and loading is required. It was found that using a well-defined sieve fraction of particles instead of fine powder minimizes errors in this respect.

As the TEOM microbalance involves flow-through operation, a second issue arises from the disruption of the sample bed due to mass losses during thermal decomposition of the HTlc (in our case up to 40%). The dynamic rearrangement of sample particles while the temperature-programmed analysis proceeds may cause undesired channelling phenomena (see illustration in Fig. 7b). Associated with this, a loose sample packing in the TEOM micro-reactor produces unstable signals due to the extreme sensitivity of the frequency measurements (not shown). In order to overcome this issue, sample bed dilution should be applied (Fig. 7c). In our experiments, mixing silicon carbide (previously calcined in static air at 1473 K for 6 h) with the sample made it possible to achieve highly reproducible results, as the hydrodynamic behaviour of the gas in the sample bed is basically

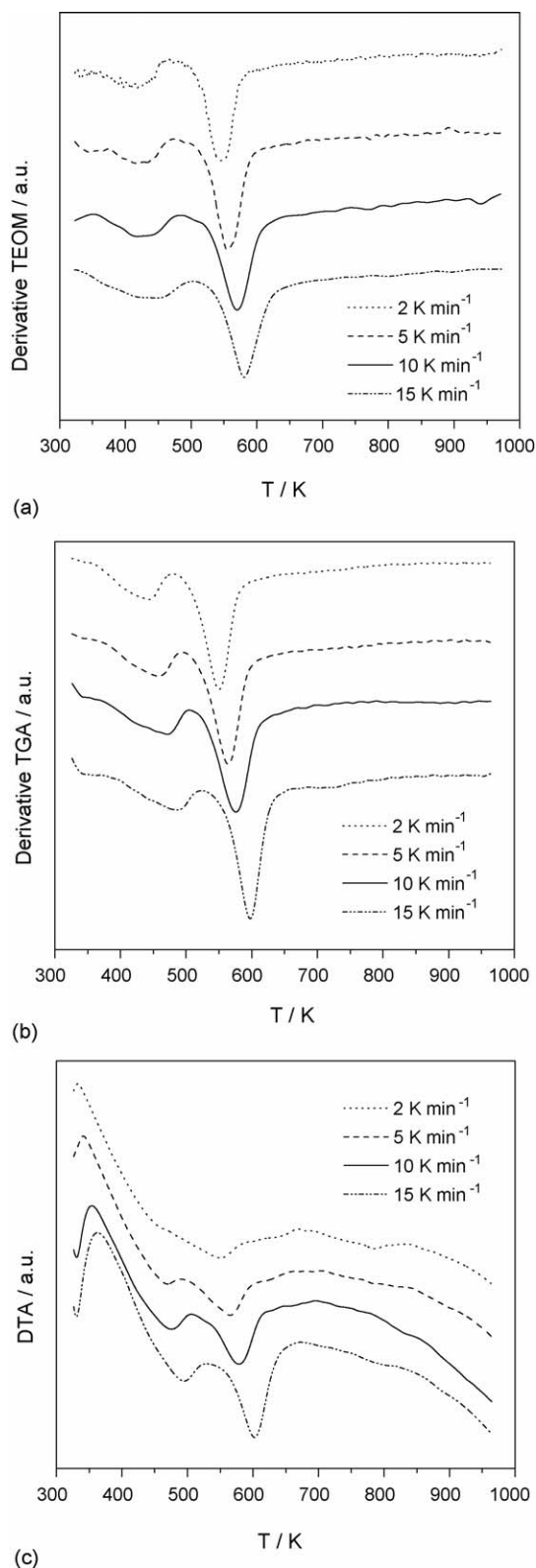


Fig. 8. First derivative of the mass loss from (a) TEOM, (b) TGA experiments, and (c) DTA profiles during decomposition of Ni-Al-HTlc-1 in air at different heating rates.

determined by the diluent. In particular, we found a volume ratio sample:diluent of 1:3 to be suitable. The same dilution ratio was applied in the TGA–DTA experiments, although it was noticed that the addition of SiC had no influence on the results repeatability.

### 3.4. Comparison of TEOM, TGA, and DTA techniques

As noted in Section 3.2, the results in Table 1 have indicated that the TEOM microbalance led to lower transition temperatures during HTlc decomposition as compared to TGA. This effect was particularly marked for the removal of interlayer water, with differences in the range of 20–30 K, but was also noticeable for dehydroxylation of the brucite-like layers and decarbonation (up to 15 K in Mg–Al-HTlc-2). In general, DTA leads to slightly higher transition temperatures than TGA. In order to gain further insights into this observation, the influence of the heating rate on the transition temperatures was also investigated over the samples. As an example, Fig. 8 shows the first derivative associated to the two transition temperatures over Ni–Al-HTlc-1 as determined by TEOM and TGA and the DTA signals at different heating rates in the range of 2–15 K min<sup>-1</sup>. As expected, the transition temperatures of the processes occurring during decomposition increase upon increasing the heating rate, which is quantified for the same sample in Fig. 9. This figure shows that the differences in transition temperatures ( $T_1$  and  $T_2$ ) between TEOM and TGA–DTA are nicely maintained in the whole range of heating rates investigated. This was also observed for the other samples and further indicates the consistency of the three methods applied.

The lower transition temperatures determined by the TEOM in comparison with TGA–DTA are likely originated by the flow-through operation in the former microbalance. This enables better mass and heat transfer properties of the reactive gas through

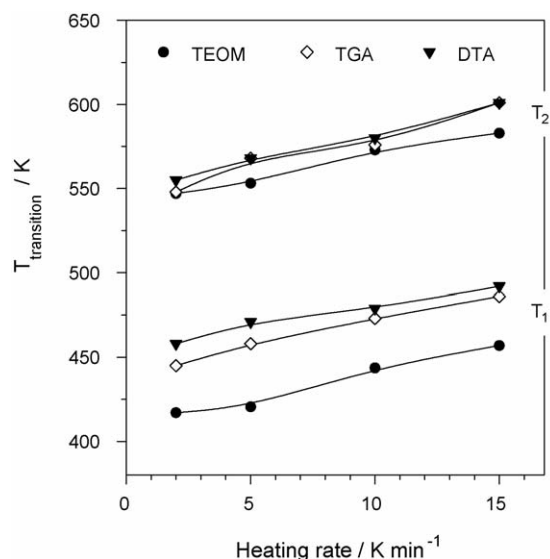


Fig. 9. Transition temperatures as determined by TEOM, TGA, and DTA during thermal decomposition of Ni–Al-HTlc-1 in air at different heating rates.  $T_1$  corresponds to dehydration by interlayer water removal and  $T_2$  corresponds to dehydroxylation and decarbonation processes, leading to the collapse of the layered structure.

the sample and an improved rejuvenation of the gaseous atmosphere around the solid as compared to the poorly defined flow patterns and creation of stagnant zones in the sample using thermogravimetric analyzers. This distinctive feature of the TEOM induces the occurrence of transitions at a lower temperature. The fact that  $T_1$  is more affected than  $T_2$  is in line with this reasoning. The former involves removal of interlayer water, being a physical process (water is stabilized in the interlayer space by means of hydrogen bonds, resulting from weak van der Waals forces) and its removal have a more marked impact on improved diffusion characteristics as compared to the second chemical transition, which involves the collapse of the layered structure of the clay and the formation of a mixed oxide phase by dehydroxylation and decarbonation.

## 4. Conclusions

Our results show that the TEOM microbalance is a suitable technique to investigate the thermal decomposition of hydrotalcites to mixed oxides. Very good agreement with well-established TGA and DTA methods has been obtained. A distinctive feature of the TEOM with respect to conventional thermogravimetric analyzers is the flow-through operation. This minimizes diffusion limitations and efficiently renews the gas in sample bed as compared to standard methods where poor gas diffusion and stagnant zones in the sample can be easily created. A consequence of this is the achievement of lower temperatures for the occurrence of associated transitions in the TEOM, mainly the removal of interlayer water but also the dehydroxylation of the brucite-like sheets and the decomposition of carbonates. The TEOM technique can be successfully applied for temperature-programmed experiments involving mass loss. However, accurate procedures for sample loading in the tapered element and bed packing are required for reproducible operation. Besides, the TEOM makes it necessary to perform blank runs for all experiments involving temperature variation.

## Acknowledgement

We thank Arne Grønvold (Hydro Research Centre Porsgrunn, Norway) for facilitating the use of the TEOM microbalance.

## References

- [1] R. Allmann, *Am. Miner.* 53 (1968) 1057–1060.
- [2] H. Taylor, *Miner. Magn.* 39 (1973) 377–389.
- [3] F. Cavani, F. Trifirò, A. Vaccari, *Catal. Today* 11 (1991) 173–301.
- [4] D. Tichit, F. Medina, B. Coq, R. Dutartre, *Appl. Catal. A* 159 (1997) 241–258.
- [5] J. Sanchez Valente, F. Figueras, M. Gravelle, P. Kumbhar, J. Lopez, J.P. Besse, *J. Catal.* 189 (2000) 370–381.
- [6] F. Millange, R.I. Walton, D. O'Hare, *J. Mater. Chem.* 10 (2000) 1713–1720.
- [7] J. Pérez-Ramírez, G. Mul, J.A. Moulijn, *Vib. Spectroscop.* 27 (2001) 75–88.
- [8] J. Pérez-Ramírez, G. Mul, F. Kapteijn, J.A. Moulijn, *J. Mater. Chem.* 11 (2001) 821–830.
- [9] W. Yang, Y. Kim, P.K.T. Liu, M. Sahimi, T. Tsotsis, *Chem. Eng. Sci.* 57 (2002) 2945–2953.

- [10] F. Hershkowitz, P.D. Madeira, *Ind. Eng. Chem. Res.* 32 (1993) 2969–2974.
- [11] D. Chen, H.P. Rebo, K. Moljord, A. Holmen, *Chem. Eng. Sci.* 51 (1996) 2687–2692.
- [12] W. Zhu, J.M. van de Graaf, L.J.P. van den Broeke, F. Kapteijn, J.A. Moulijn, *Ind. Eng. Chem. Res.* 37 (1998) 1934–1942.
- [13] S. van Donk, A. Broersma, O.L.J. Gijzeman, J.A. van Bokhoven, J.H. Bitter, K.P. de Jong, *J. Catal.* 204 (2001) 272–280.
- [14] T. Sperle, D. Chen, R. Lodeng, A. Holmen, *Appl. Catal. A* 282 (2005) 195–204.
- [15] N.H. Jalani, C. Pyoungho, R. Datta, *J. Membr. Sci.* 254 (2005) 31–38.
- [16] X. Xu, C. Song, *Appl. Catal. A* 300 (2006) 130–138.
- [17] J. Pérez-Ramírez, A. Gallardo-Llamas, C. Daniel, C. Mirodatos, *Chem. Eng. Sci.* 59 (2004) 5535–5543.
- [18] W.T. Reichle, S.Y. Kang, D.S. Everhardt, *J. Catal.* 101 (1986) 352–359.